Scientific Research Publishing

Pharmacology & Pharmacy, 2022, 13, 174-188
https://www.scirp.org/journal/pp
ISSN Online: 2157-9431
ISSN Print: 2157-9423

Synthesis, Photophysical Properties and DNA-Photocleavage Activity of Silicon Phthalocyanine Derivatives

Kunhui Sun, Yanli Ge*, Jun Yang, Xuelei Hu

Key Laboratory for Green Chemical Process of Ministry of Education, School of Chemical Engineering and Pharmacy, Wuhan Institute of Technology, Wuhan, China
Email: *sunbird80@126.com

How to cite this paper: Sun, K.H., Ge, Y.L., Yang, J. and Hu, X.L. (2022) Synthesis, Photophysical Properties and DNA-Photocleavage Activity of Silicon Phthalocyanine Derivatives. *Pharmacology & Pharmacy*, **13**, 174-188.
https://doi.org/10.4236/pp.2022.136014

Received: May 7, 2022
Accepted: June 27, 2022
Published: June 30, 2022

Abstract

Silicon phthalocyanine derivatives 1a and 1b were synthesized and characterized by UV, ^{1}H-NMR and MS. The photophysical properties of the compounds in DMSO were investigated. The maximum absorption peaks of compounds 1a and 1b at the Q-band are 681 nm. With ZnPc (Φ_F = 0.20, Φ_Δ = 0.67) as a reference, the fluorescence quantum yield (Φ_F) of 1a and 1b are 0.20 and 0.31 respectively, and the singlet oxygen quantum yield (Φ_Δ) are 0.66 and 0.59 respectively. The DNA-photocleavage activities of compounds 1a and 1b were studied by gel electrophoresis. Compounds 1a and 1b possess good photocleavage activity to pBR322 DNA. The results demonstrate that compounds 1a and 1b are potential photosensitizers for tumor therapy.

Keywords

Silicon Phthalocyanine, Fluorescence Quantum Yield, Singlet Oxygen Quantum Yield, DNA-Photocleavage Activity

1. Introduction

Photodynamic therapy (PDT) has attracted much attention as a promising treatment modality for some cancers [1] [2] [3] [4] [5]. In the PDT process, a nontoxic photosensitizer will preferentially accumulate in tumor cells or their vasculature. After photoirradiation at a specific wavelength [6] [7] [8] [9], these photosensitizers will produce cytotoxic reactive oxygen species (ROS), principally singlet oxygen ($^1O_2$), which then kills the tumor cells [10] [11]. Photosensitizers that localize to mitochondria are considered more interesting for killing cells than those localizing at other cellular sites because they can cause cell death

by apoptosis [12] [13]. It was reported that delocalized lipophilic cations inherently share the ability to cross the mitochondrial membranes and target the mitochondria [14].

Phthalocyanines have been widely studied as potential PDT agents due to their tumor-localizing properties, photophysical and photochemical properties and modifiable structure [15] [16] [17]. The solubility of phthalocyanines is very important for biological studies. The water solubility of phthalocyanine can be constructed by the introduction of hydrophilic substituents, such as sulfonate [18], N-methylimidazo-lium [14] and N-methylpyridinium [19].

In this paper, two silicon phthalocyanine derivatives were designed based on the idea that a phthalocyanine substituted with 1-(N-methyl) imidazoliumyl-ethyloxy or 2-(N-methyl) pyridyl-ethyloxy should possess the characteristics of a lipophilic cation, namely, be preferentially localized to the mitochondria. Additionally, the introduction of a quaternary ammonium salt can greatly enhance the aqueous solubility of phthalocyanines. The synthesis, photophysical properties and DNA-photocleavage activity of silicon phthalocyanine derivatives 1a and 1b (Scheme 1) are reported herein.

2. Experimental Section

2.1. Reagents and Apparatus

Experimental details Silicon (IV) phthalocyanine dichloride ($SiPcCl_2$) was synthesized by a reported procedure [20]. All other solvents and reagents were commercially available and were used without further purification. NMR spectra were recorded with a Varian Mercury 300 spectrometer. Mass spectra were recorded with IonSpec 4.7 Tesla FT mass spectrometer. Electronic absorption spectra in the UV-Vis region were measured with a UV-2450 spectrophotometer. Fluorescence spectra were collected with RF-5301PC fluorescence spectrometer.

2.2. Synthesis of Bis[2-(1-imidazolyl) ethoxy] silicon phthalocyanine (2a)

A mixture of $SiPcCl_2$ (0.50 g, 0.82 mmol), 1-(2-hydroxyethyl)imidazole (0.74 g,

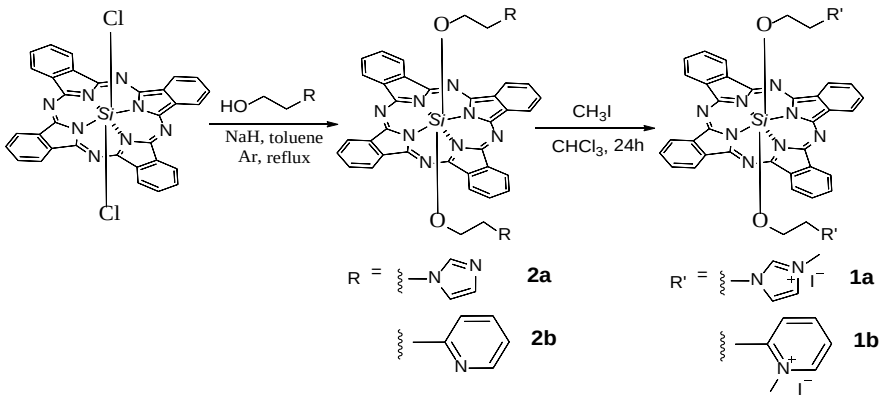

Scheme 1. Synthesis of the target compounds 1a and 1b.

6.56 mmo1), and NaH (0.10 g, 8.2 mmol) in toluene (20 mL) were refluxed for 24 h. After evaporating the solvent in vacuo, the residue was dissolved in excess $CHCl_3$. The mixture was filtered and the filtrate was concentrated under reduced pressure. The residue was successively washed with water, acetone and dichloromethane, and purified by recrystallization with chloroform/petroleum ether to give 2a as a dark blue solid (0.18 g), yielding 29.4%. ^{1}H-NMR (300 MHz, $CDCl_3$, ppm): δ = 9.543 - 9.672 (m, 8H, Pc), 8.381 - 8.409 (m, 8H, Pc), 5.974 (s, 2H, imidazole), 5.279 (s, 2H, imidazole), 4.342 (s, 2H, imidazole), 0.969 (t, J = 5.1 Hz, 4H, CH_2), −1.887 (t, J = 5.1 Hz, 4H, CH_2-O). ESI-MS: m/z 763.5 for $[M + H]^+$, 651.2 for $[M\text{-}O\text{-}CH_2\text{-}CH_2\text{-imidazole}]^+$.

Synthesis of Bis[2-(2-pyridyl) ethoxy] silicon phthalocyanine (2b): According to the above procedure, $SiPcCl_2$ (0.50 g, 0.82 mmol) was treated with 2-hydroxyethylpyridine (0.8 mL, 6.56 mmo1), and NaH (0.10 g, 8.2 mmol) in toluene (20 mL) to give 2b as a dark blue solid (0.22 g), yield 34.3%. ^{1}H-NMR (300 MHz, $CDCl_3$, ppm): δ = 9.554 - 9.582 (m, 8H, Pc), 8.329 - 8.356 (m, 8H, Pc), 7.455 (d, J = 1.8 Hz, 2H, pyridine), 6.412 - 6.550 (m, 4H, pyridine), 4.274 (d, J = 3.6 Hz, 2H, pyridine), −0.083 (t, J = 5.7 Hz, 4H, CH_2), −1.834 (t, J = 5.1 Hz, 4H, CH_2-O). ESI-MS: m/z 785.3 for $[M + H]^+$, 662.1 for $[M\text{-}O\text{-}CH_2\text{-}CH_2\text{-pyridine}]^+$.

2.3. Synthesis of Bis[2-(1-(N-methyl) imidazolyl) ethoxy] silicon phthalocyanine diiodide (1a)

A mixture of compound 2a (0.50 g, 0.65 mmol) and a large excess of methyl iodide (0.4 mL) in chloroform (20 mL) was stirred for 24 h at room temperature. The mixture was filtered, and the solvent and excess methyl iodide as the filtrate were removed. The crude product was washed successively with chloroform and acetone and dried in a vacuum. Compound 1a was obtained as a dark blue solid (0.50 g), yielding 73.1%. ^{1}H-NMR (300 MHz, DMSO-d_6, ppm): δ = 9.691 - 9.720 (m, 8H, Pc), 8.565 - 8.592 (m, 8H, Pc), 6.685 (s, 2H, imidazole), 6.576 (s, 2H, imidazole), 5.493 (s, 2H, imidazole), 3.426 (s, 6H, CH_3), 1.361 (s, 4H, CH_2), −1.988 (s, 4H, OCH_2). ESI-MS: m/z 919.7 for $[M - I]^+$, 396.5 for $[M - 2I]^{2+}$.

Synthesis of Bis[2-(2-(N-methyl) pyridyl) ethoxy] silicon phthalocyanine diiodide (1b): According to the above procedure, compound 2a (0.68 g, 0.65 mmol) was treated with a large excess of methyliodide (0.4 mL) in chloroform (20 mL) to give 1b as a dark blue solid (0.71 g), yield 68.3%. ^{1}H-NMR (300 MHz, DMSO-d_6, ppm): δ = 9.619 - 9.626 (m, 8H, Pc), 8.578 - 8.595 (m, 8H, Pc), 7.811 (d, J = 2.7 Hz, 2H, pyridine), 7.325 - 7.441 (m, 4H, pyridine), 5.671 (d, J = 3.9 Hz, 2H, pyridine), 1.738 (s, 6H, CH_3), 0.438 (s, 4H, CH_2), −1.858 (s, 4H, OCH_2). ^{13}C-NMR (75 MHz, DMSO-d_6): δ = 147.7, 133.3, 132.8, 130.7, 122.3, 120.6, 118.0, 52.4, 46.3, 33.7. ESI-MS: m/z 941.6 for $[M - I]^+$, 799.5 for $[M - Me - 2I]^+$, 407.5 for $[M - 2I]^{2+}$.

2.4. UV-vis Absorption Spectra of Compounds 1a-1b

The compound storage solution (10 mM) was diluted 10 times with DMSO to a

1 mM solution, and then the solution (1 mM, 2 μL) was diluted with DMSO to a final concentration (5 μM, 400 μL). Six test concentrations (5 μM, 4 μM, 3 μM, 2 μM, 1 μM, and 0.5 μM) were prepared by the stepwise dilution method. Using DMSO as a blank reference, the UV-Vis absorption spectra of compounds in DMSO at room temperature were measured with a UV-2450 spectrophotometer.

2.5. Fluorescence Spectra of Compounds 1a-1b

The test solutions of compounds 1a-1b and ZnPc in DMSO at different concentrations (5 μM, 4 μM, 3 μM, 2 μM, 1 μM, and 0.5 μM) were prepared by the stepwise dilution method. The fluorescence emission spectra of the compounds at room temperature were collected with RF-5301PC fluorescence spectrometer, and the slit width was set as Ex = 3.0 and Em = 3.0, the excitation wavelength was 610 nm.

2.6. Singlet Oxygen Quantum Yields of Compounds 1a-1b

To evaluate the photosensitizing efficiency of compounds 1a and 1b, their singlet oxygen quantum yields (Φ_{Δ}) were determined in DMSO by a steady-state method with 1,3-diphenylisobenzofuran (DPBF) as the scavenger [21]. DMSO solutions containing compounds 1a, 1b or ZnPc (0.2 μM) and DPBF (50 μM) were prepared in the dark. The DMSO solutions were irradiated with a 150 W halogen lamp at a distance of 15 cm, and then the photooxidation of DPBF was monitored at an interval of 10 s up to 90 s.

2.7. DNA-Photocleavage Activity of Compounds 1a-1b

The DNA-photocleavage activity of compounds 1a and 1b was studied using supercoiled pBR322 DNA (0.05 μg) in a Tris-HCl/EDTA (TE, 10 mM, pH 7.5) buffer on irradiation with a 150 W halogen lamp at a distance of 15 cm. After light exposure, each sample was analyzed by agarose (0.9%) gel electrophoresis.

3. Results and Discussion

3.1. Photophysical Properties of Compounds 1a-1b

The UV-vis absorption spectra of compounds 1a and 1b in DMSO were typical of the spectra of nonaggregated phthalocyanines (**Figure S1** in the Supporting Information), showing intense absorption peaks in the Soret-band (B-band) and Q-band regions, with the Q-band having a vibrational peak at its higher energy. The electron absorption peaks and molar extinction coefficients (ε) of compounds 1a and 1b are shown in **Table 1**.

Upon excitation at 610 nm, the compounds show a fluorescence emission at 688 nm for 1a and 683 nm for 1b (**Figure S2** in the Supporting Information). Using ZnPc as the reference, the fluorescence quantum yield (Φ_F) of compounds was calculated using Equation (1) [22]:

$$\Phi_{F(\text{sample})} = (F_{\text{sample}}/F_{\text{ref}})\cdot(A_{\text{ref}}/A_{\text{sample}})\cdot\Phi_{F(\text{ref})} \quad (1)$$

Table 1. Photophysical properties of compound 1a and 1b in DMSO.

Compd.	Absorption peaks (nm) [ε ($M^{-1}\cdot cm^{-1}$)]			λ_{Em} (nm)[a]	Φ_F[b]	Φ_Δ[b]
	B-band	Q-band (λ_{vib})	Q-band (λ_{max})			
1a	357 [6.871 × 104]	612 [3.623 × 104]	681 [2.179 × 105]	688	0.20	0.66
1b	357 [5.214 × 104]	613 [2.732 × 104]	681 [1.608 × 105]	683	0.31	0.59

[a]Excited at 610 nm. [b]Using ZnPc in DMSO as the reference (Φ_F = 0.2, Φ_Δ = 0.67).

where $\Phi_{F(ref)}$ is the fluorescence quantum yield for ZnPc ($\Phi_{F(ZnPc)}$ = 0.2 in DMSO [23]), Fsample and Fref are the areas under the fluorescence emission curves of the phthalocyanine and ZnPc, respectively. Asample and Aref are the absorbances of the phthalocyanine and ZnPc at the excitation wavelengths, respectively.

From the areas under the fluorescence emission curves (**Figure S2**), the fluorescence quantum yield (Φ_F) was calculated as 0.20 for compound 1a and 0.31 for compound 1b (**Table 1**).

3.2. Singlet Oxygen Quantum Yields of Compounds 1a-1b

The decrease in the absorption of DPBF was monitored at 416 nm as shown in **Figure 1**, which is due to the compound sensitized generation of singlet oxygen followed by photooxidation of DPBF. Using ZnPc as the reference, the singlet oxygen quantum yields (Φ_Δ) of compounds were calculated using the equation 2 [22]:

$$\Phi_{\Delta(sample)} = (K_{sample}/K_{ref})\cdot(A_{ref}/A_{sample})\cdot\Phi_{\Delta(ref)} \quad (2)$$

where $\Phi_{\Delta(ref)}$ is the singlet oxygen quantum yield for ZnPc ($\Phi_{\Delta(ZnPc)}$ = 0.67 in DMSO [23]), Ksample and Kref are the DPBF photobleaching rates in the presence of the phthalocyanine and ZnPc, respectively. Asample and Aref are the integrated areas of the Q-band absorption peak of the phthalocyanine and ZnPc in the wavelength range of 610 - 800 nm, respectively.

From the slope of the graph obtained by plotting the change in optical density against the time interval (**Figure 2**), the singlet oxygen quantum yields were calculated as 0.66 for compound 1a and 0.59 for compound 1.

3.3. DNA-Photocleavage Activity of Compounds 1a-1b

Photocleavage activities of supercoiled pBR322 DNA (0.05 μg) by compound 1a or 1b (10 μM) with different illumination times were shown in **Figure 3**. Compounds 1a and 1b with light irradiation can cleave supercoiled DNA (Form I) to nicked DNA (Form II), and the photocleavage activities increase with the prolongation of illumination time. To avoid prolonged exposure of DNA to air, it is considered the optimal illumination time is 35 minutes. Photocleavage activities of supercoiled pBR322 DNA (0.05 μg) by compound 1a or 1b in different concentrations with light irradiation for 35 min were shown in **Figure 4**. Compounds 1a and 1b at a concentration of 20 μM show significant photo-induced DNA cleavage activities.

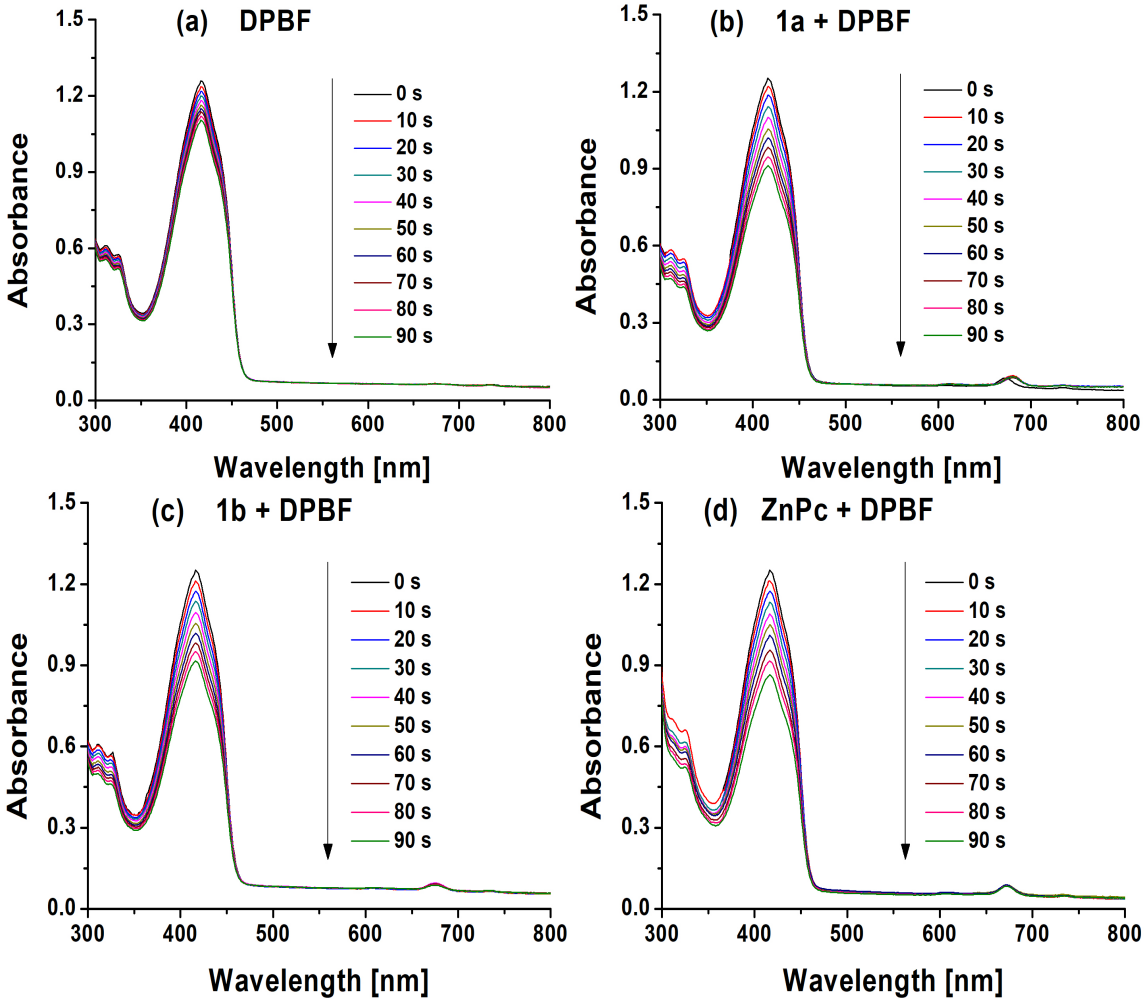

Figure 1. Absorption spectra of DPBF (50 μM) in the presence or absence of compound (2 μM) in DMSO at different illumination times. (a) DPBF, (b) 1a + DPBF, (c) 1b + DPBF, (d) ZnPc + DPBF.

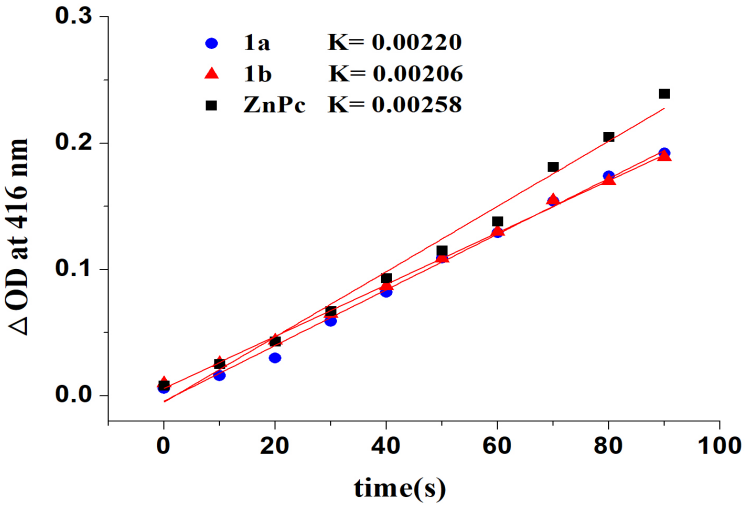

Figure 2. Plot of change in absorbance of DPBF (50 μM) at 416 nm vs different irradiation time in the presence of compound 1a or 1b (0.2 μM) versus ZnPc (0.2 μM) as the reference in DMSO.

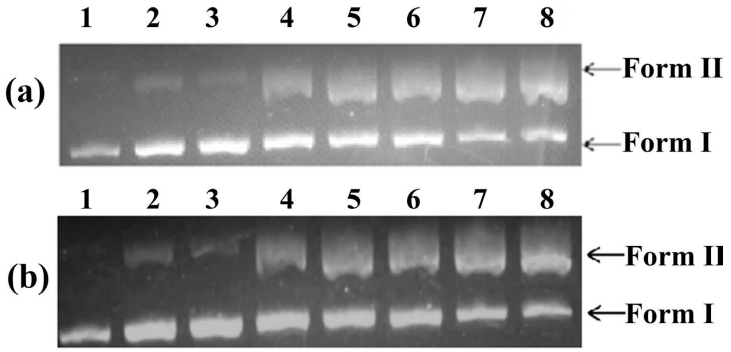

Figure 3. Photocleavage activities of supercoiled pBR322 DNA (0.05 μg) by compound 1a (a) or 1b (b) (10 μM) with different illumination time (10 μL mixtures). Lane 1: DNA in dark, Lane 2: DNA + light irradiation for 40 min, Lane 3 - 8: compound (10 μM), Lane 3: DNA, Lane 4: DNA + light irradiation for 10 min, Lane 5: DNA + light irradiation for 20 min, Lane 6: DNA + light irradiation for 30 min, Lane 7: DNA + light irradiation for 35 min, Lane 8: DNA + light irradiation for 40 min.

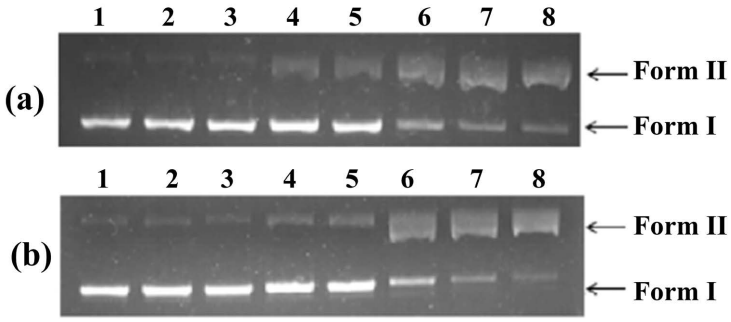

Figure 4. Photocleavage activities of supercoiled pBR322 DNA (0.05 μg) by compound 1a (a) or 1b (b) in different concentration (10 μL mixtures) with light irradiation for 35 min. Lane 1: DNA in dark, Lane 2: DNA + light irradiation for 35 min, Lane 3: DNA + compound (25 μM) in dark, Lane 4 - 8: light irradiation for 35 min, Lane 4: DNA + compound (0.5 μM), Lane 5: DNA + compound (1 μM), Lane 6: DNA + compound (10 μM), Lane 7: DNA + compound (20 μM), Lane 8: DNA + compound (25 μM).

4. Conclusion

In summary, we synthesized and characterized two silicon phthalocyanine derivatives 1a and 1b, and evaluated their photophysical properties in DMSO and DNA-photocleavage activities. The maximum absorption peaks of compounds 1a and 1b at the Q-band are 681 nm. With ZnPc (Φ_F = 0.20, Φ_Δ = 0.67) as a reference, the fluorescence quantum yield (Φ_F) of 1a and 1b are 0.20 and 0.31 respectively, and the singlet oxygen quantum yield (Φ_Δ) are 0.66 and 0.59 respectively. Compounds 1a and 1b possess good photocleavage activity to pBR322 DNA. The above results show that two silicon phthalocyanine derivatives are promising antitumor agents for photodynamic therapy.

Acknowledgements

This research was supported by the Open Fund of the Key Laboratory of Green Chemical Process Education Ministry of Education (No. 2017001), Scientific

Research Fund of Wuhan University of Technology (No. K201435).

Conflicts of Interest

The authors declare no conflicts of interest regarding the publication of this paper.

References

[1] Li, X., Zheng, B.D., Peng, X.H., Li, S.Z., Ying, J.W., Zhao, Y., *et al.* (2017) Phthalocyanines as Medicinal Photosensitizers: Developments in the Last Five Years. *Coordination Chemistry Reviews*, **379**, 147-160. https://doi.org/10.1016/j.ccr.2017.08.003

[2] Lim, C., Sim, T., Hoang, N.H., Jung, C.E., Lee, E.S., Youn, Y.S., *et al.* (2017) A Charge-Reversible Nanocarrier Using PEG-PLL (-g-Ce6, DMA)-PLA for Photodynamic Therapy. *International Journal of Nanomedicine*, **12**, 6185-6196. https://doi.org/10.2147/IJN.S142912

[3] Wang, C., Wang, S.D., Wang, Y., Wu, H., Bao, K., Sheng, R. and Li, X. (2020) Microenvironment-Triggered Dual-Activation of a Photosensitizer-Fluorophore Conjugate for Tumor Specific Imaging and Photodynamic Therapy. *Scientific Reports*, **10**, Article No. 12127. https://doi.org/10.1038/s41598-020-68847-w

[4] Michy, T., Massias, T., Bernard, C., Vanwonterghem, L., Henry, M., Guidetti, M., *et al.* (2019) Verteporfin-Loaded Lipid Nanoparticles Improve Ovarian Cancer Photodynamic Therapy *in Vitro* and *in Vivo*. *Cancers*, **11**, Article ID: 1760. https://doi.org/10.3390/cancers11111760

[5] Gadzinski, J.A., Guo, J., Philips, B.J., Basse, P., Craig, E.K., Bailey, L., *et al.* (2016) Evaluation of Silicon Phthalocyanine 4 Photodynamic Therapy Against Human Cervical Cancer Cells *in Vitro* and in Mice. *Advances in Biological Chemistry*, **6**, 193-215. https://doi.org/10.4236/abc.2016.66017

[6] Liu, Q., Pang, M., Tan, S., Wang, J., Chen, Q., Wang, K., *et al.* (2018) Potent Peptide-Conjugated Silicon Phthalocyanines for Ttumor Photodynamic Therapy. *Journal of Cancer*, **9**, 310-320. https://doi.org/10.7150/jca.22362

[7] Zhang, Y., Ng, D.K.P. and Fong, W.P. (2019) Antitumor Immunity Induced by The Photodynamic Action of BAM-SiPc, A Silicon (IV) Phthalocyanine Photosensitizer. *Cellular & Molecular Immunology*, **16**, 676-678. https://doi.org/10.1038/s41423-019-0239-8

[8] Kobayashi, H. and Choyke, P.L. (2019) Near-Infrared Photoimmunotherapy of Cancer. *Accounts of Chemical Research*, **52**, 2332-2339. https://doi.org/10.1021/acs.accounts.9b00273

[9] Sarı, C., Nalçaoğlu, A., Değirmencioğlu, İ. and Eyüpoğlu, F.C. (2021) Tumor-Selective New PiperaZine-Fragmented Silicon Phthalocyanines Initiate Cell Death in Breast Cancer Cell Lines. *Journal of Photochemistry and Photobiology B: Biology*, **216**, Article ID: 112143. https://doi.org/10.1016/j.jphotobiol.2021.112143

[10] Westover, D. and Li, F.Z. (2015) New Trends for Overcoming ABCG2/BCRP-Mediated Resistance to Cancer Therapies. *Journal of Experimental & Clinical Cancer Research*, **34**, Article No. 159. https://doi.org/10.1186/s13046-015-0275-x

[11] Amirshaghaghi, A., Yan, L., Miller, J., Daniel, Y., Stein, J.M., Busch, T.M., Cheng, Z.L. and Tsourkas, A. (2019) Chlorin e6-Coated Superparamagnetic Iron Oxide Nanoparticle (SPION) Nanoclusters as a Theranostic Agent for Dual-Mode Imaging and Photodynamic Therapy. *Scientific Reports*, **9**, Article No. 2613. https://doi.org/10.1038/s41598-019-39036-1

[12] Fulda, S., Galluzzi, L. and Kroemer, G. (2010) Targeting Mitochondria for Cancer Therapy. *Nature Reviews Drug Discovery*, **9**, 447-464. https://doi.org/10.1038/nrd3137

[13] Yousif, L.F., Stewart, K.M. and Kelley, S.O. (2009) Targeting Mitochondria with Organelle-Specific Compounds: Strategies and Applications. *ChemBioChem*, **10**, 1939-1950. https://doi.org/10.1002/cbic.200900185

[14] Ge, Y., Weng, X., Tian, T., Ding, F., Huang, R., Yuan, L., *et al.* (2013) A Mitochondria-Targeted Zinc(II) Phthalocyanine for Photodynamic Therapy. *Royal Society of Chemistry Advances*, **3**, 12839-12846. https://doi.org/10.1039/c3ra41647j

[15] Huang, M., Chen, Z., Chen, J. and Iqbal, Z. (2015) Phthalocyanine-Biomolecule Conjugated Photosensitizers for Targeted Photodynamic Therapy and Imaging. *Current Drug Metabolism*, **16**, 816-832. https://doi.org/10.2174/1389200217666151120165404

[16] Hadi, L.M., Yaghini, E., Macrobert, A.J. and Loizidou, M. (2020) Synergy between Photodynamic Therapy and Dactinomycin Chemotherapy in 2D and 3D Ovarian Cancer Cell Cultures. *International Journal of Molecular Sciences*, **21**, Article No. 3203. https://doi.org/10.3390/ijms21093203

[17] Portilho, F.A., Cavalcanti, C., Miranda-Vilela, A.L., Estevanato, L. and Lacava, Z. (2013) Antitumor Activity of Photodynamic Therapy Performed with Nanospheres Containing Zinc-Phthalocyanine. *Journal of Nanobiotechnology*, **11**, Article No. 41. https://doi.org/10.1186/1477-3155-11-41

[18] Cauchon, N., Tian, H., Langlois, R., La Madeleine, C., Martin, S., Ali, H., *et al.* (2005) StructurePhotodynamic Activity Relationships of Substituted Zinc Trisulfophthalocyanines. *Bioconjugate Chemistry*, **16**, 80-89. https://doi.org/10.1021/bc049848t

[19] Kuznetsova, N., Makarov, D., Yuzhakova, O., Strizhakov, A., Roumbal, Y., Ulanova, L., *et al.* (2009) Photophysical Properties and Photodynamic Activity of Octacationic Oxotionic Oxotitanium(IV) Phthalocyanines. *Photochemical and. Photobiological Sciences*, **8**, 1724-1733. https://doi.org/10.1039/b9pp00054b

[20] Ke, L., Gasparini, N., Min, J., Zhang, H., Adam, M., Rechberger, S., *et al.* (2017) Panchromatic Ternary/Quaternary Polymer/Fullerene BHJ Solar Based on Novel Silicon Naphthalocyanine and Silicon Phthalocyanine Dye Sensitizers. *Journal of Materials Chemistry A*, **5**, 2550-2562. https://doi.org/10.1039/C6TA08729A

[21] Jiang, X.J., Yeung, S.L., Lo, P.C., Fong, W.P. and Ng, D.K. (2011) Phthalocyanine-Polyamine Conjugates as Highly Efficient Photosensitizers for Photodynamic Therapy. *Journal of Medicinal Chemistry*, **54**, 320-330. https://doi.org/10.1021/jm101253v

[22] Nascimento, F.B.D. and Ribeiro, A.O. (2017) Investigation of Synthetic Pathways of CarbOxylic Acid Pathalocyanines from Glycolic and Lactic Acids. *Inorganica. Chimica Acta*, **467**, 106-116. https://doi.org/10.1016/j.ica.2017.07.053

[23] Bıyıklıoğlu, Z., Durmu, M. and Kantekin, H. (2011) Tetra-2-[2-(Dimethylamino)-Ethoxy] Ethoxy Substituted Zinc Phthalocyan-ines and Their Quaternized Analoques: Syntheisis, Characterization, Photophysical and Photochemical Properties. *Journal of Photochemistry and Photobiology A*: *Chemistry*, **222**, 87-96. https://doi.org/10.1016/j.jphotochem.2011.05.006

Supporting Information

^{1}H-NMR, ^{13}C-NMR and MS spectra of all new compounds, absorption and fluorescence spectra for compounds 1a and 1b in DMSO.

Synthesis, Photophysical Properties and DNA-photocleavage Activity of Silicon Phthalocyanine Derivatives

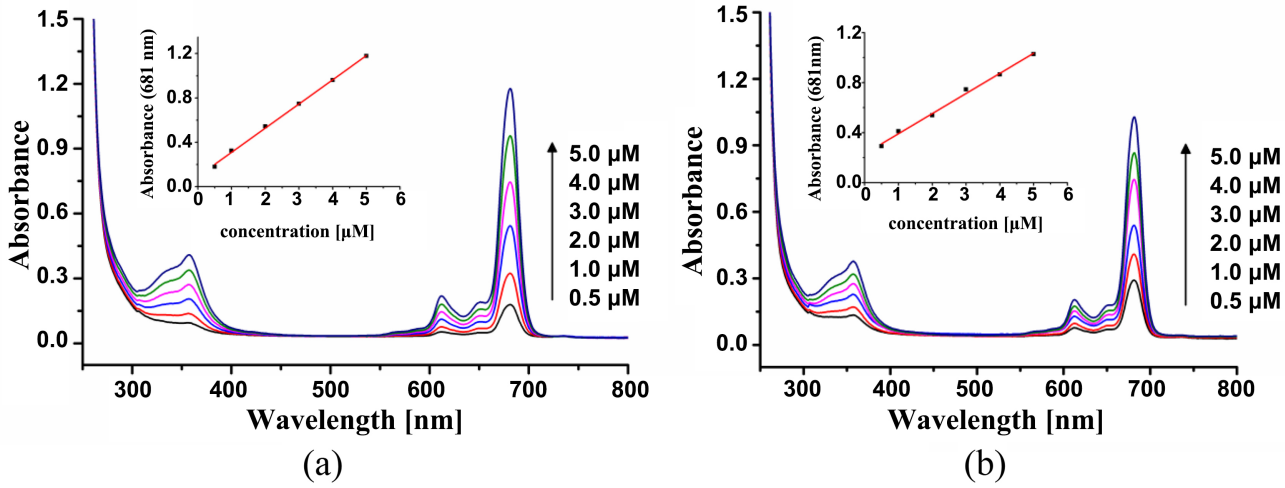

Figure S1. UV-Vis absorption spectra of compounds 1a (a) and 1b (b) in DMSO at different concentrations. The inset plots the absorbance at 681 nm (λ_{max}) versus the concentration of the compound.

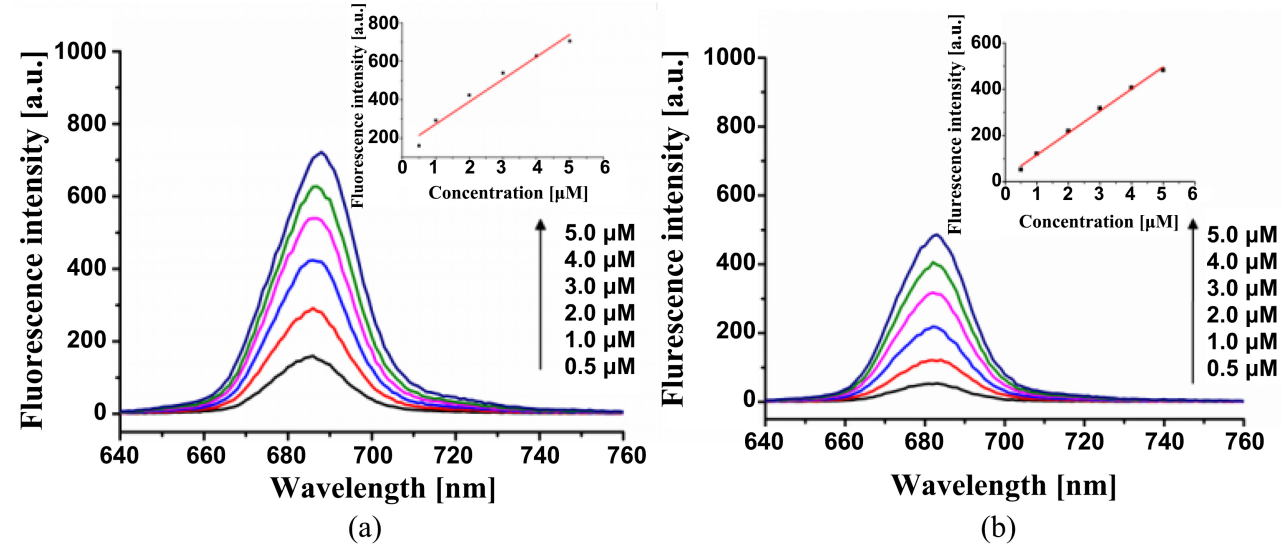

Figure S2. Fluoresence emission spectra of compounds 1a (a) and 1b (b) in DMSO at different concentrations (λ_{Ex} = 610 nm).

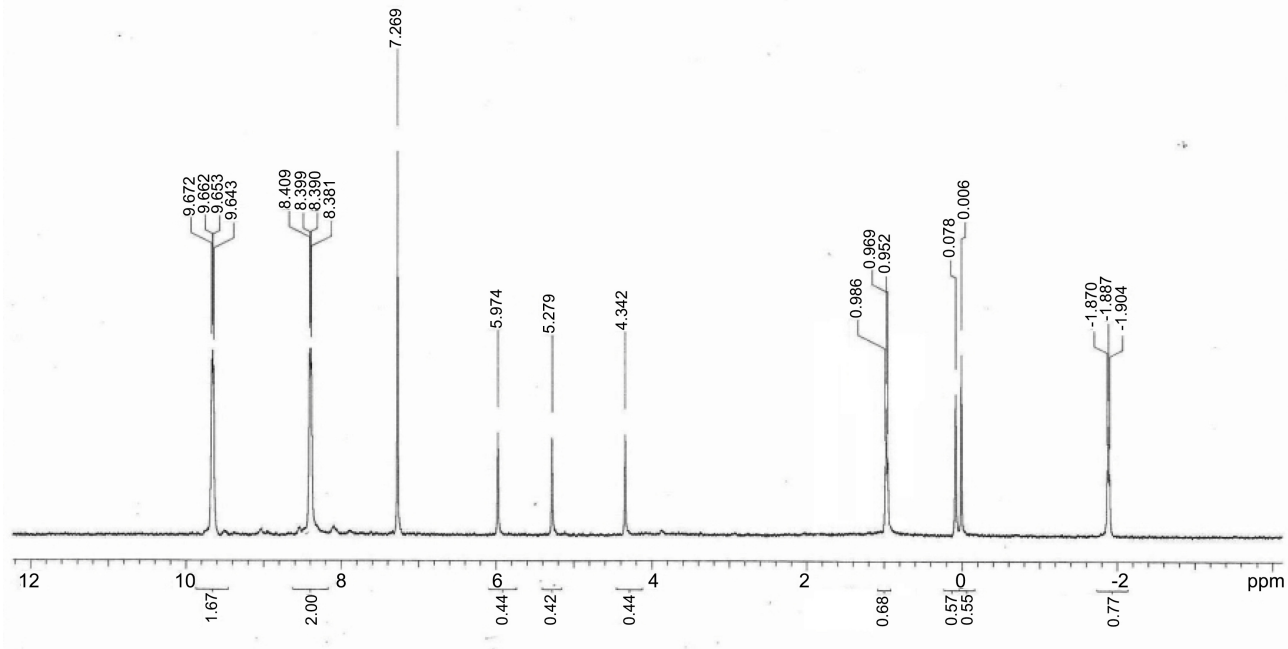

Figure S3. ^{1}H NMR spectrum of compound 2a in $CDCl_3$.

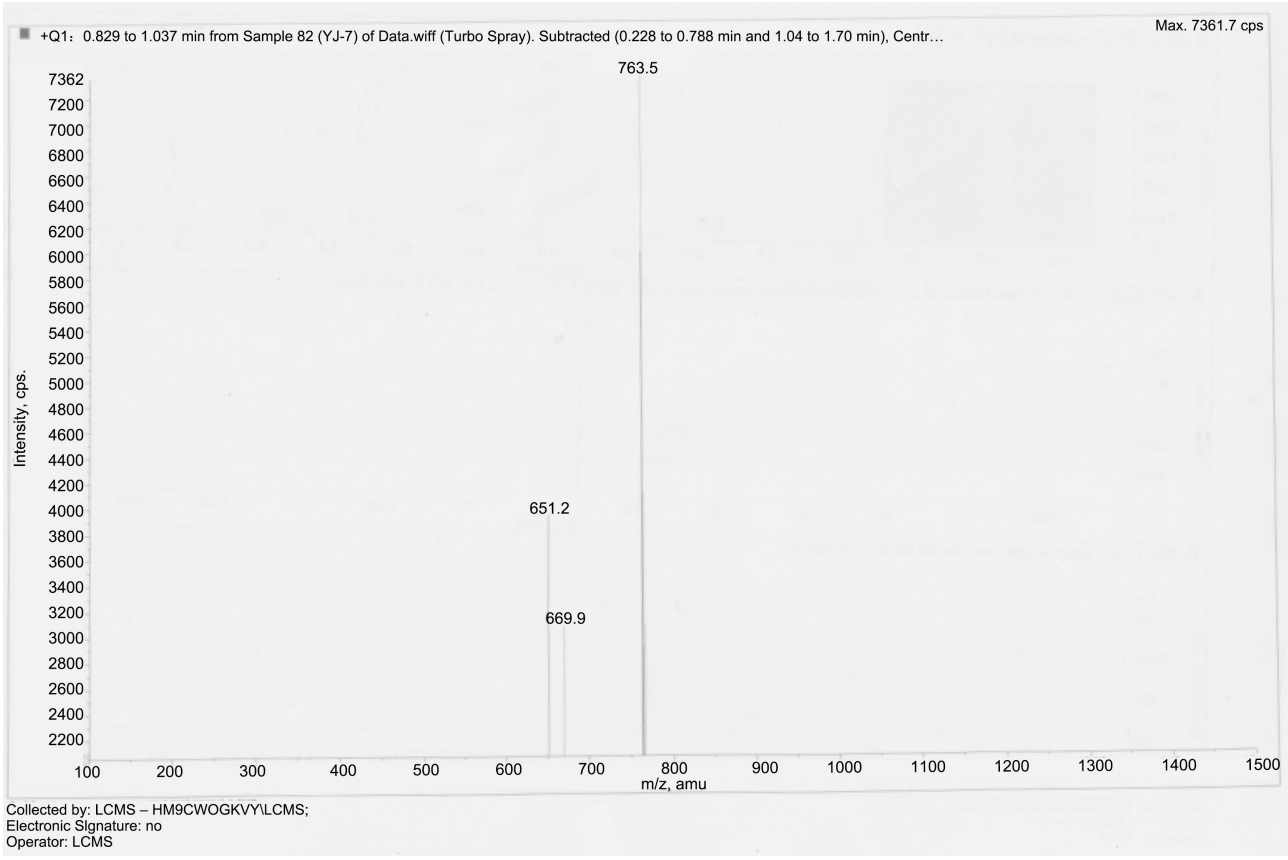

Figure S4. MS spectrum of compound 2a.

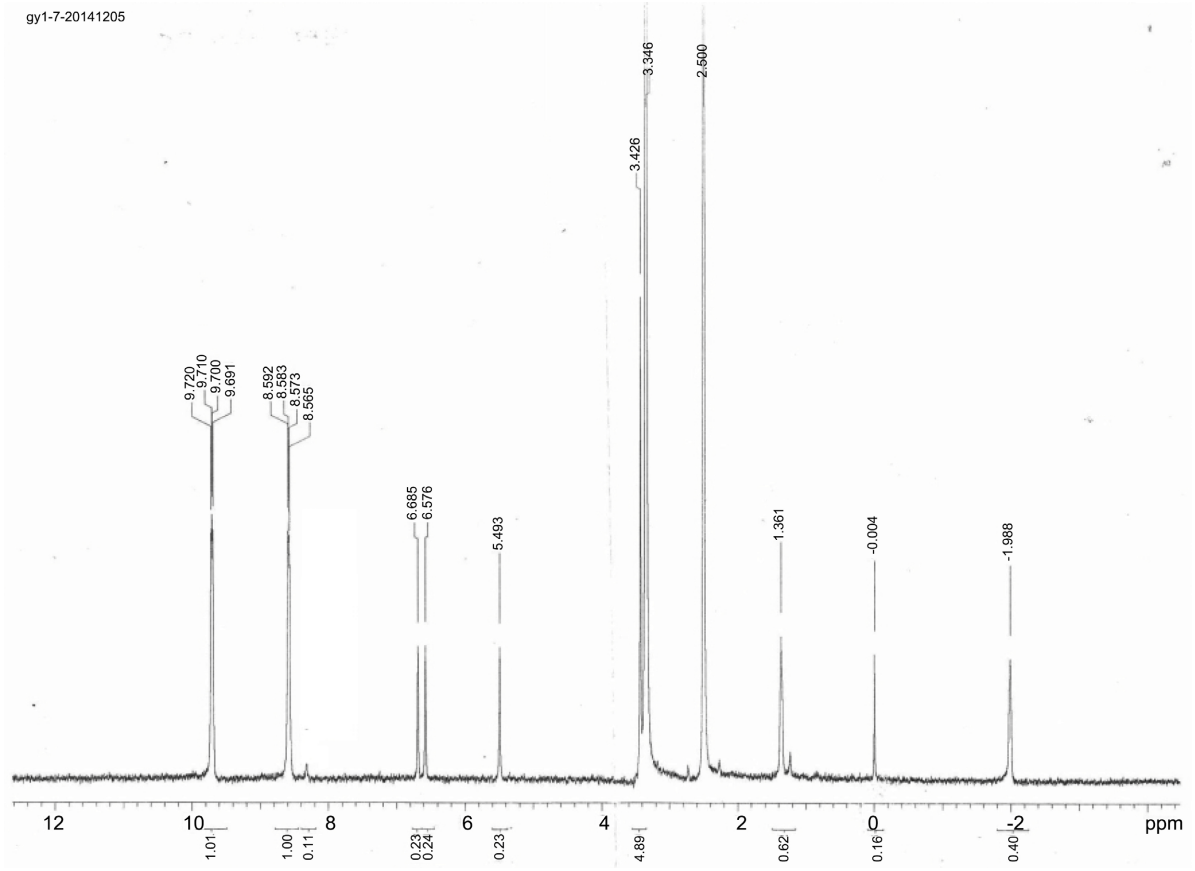

Figure S5. ^{1}H NMR spectrum of compound 1a in DMSO-d_6.

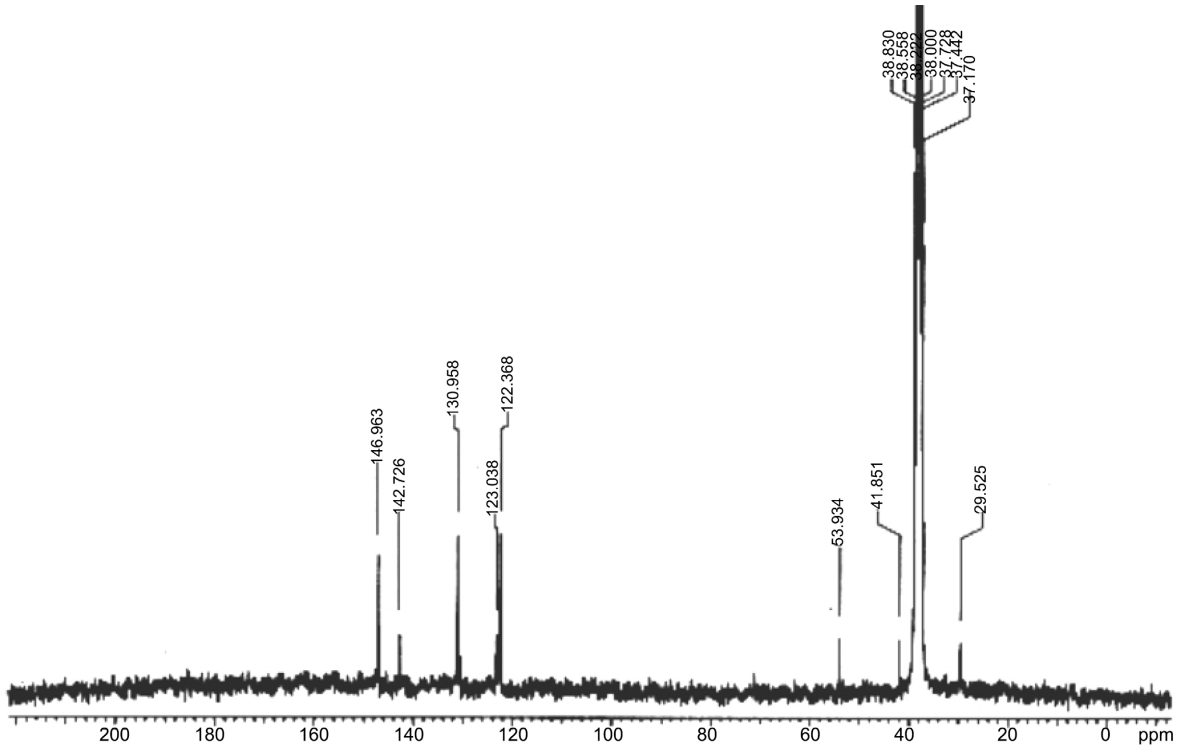

Figure S6. ^{13}C NMR spectrum of compound 1a in DMSO-d_6.

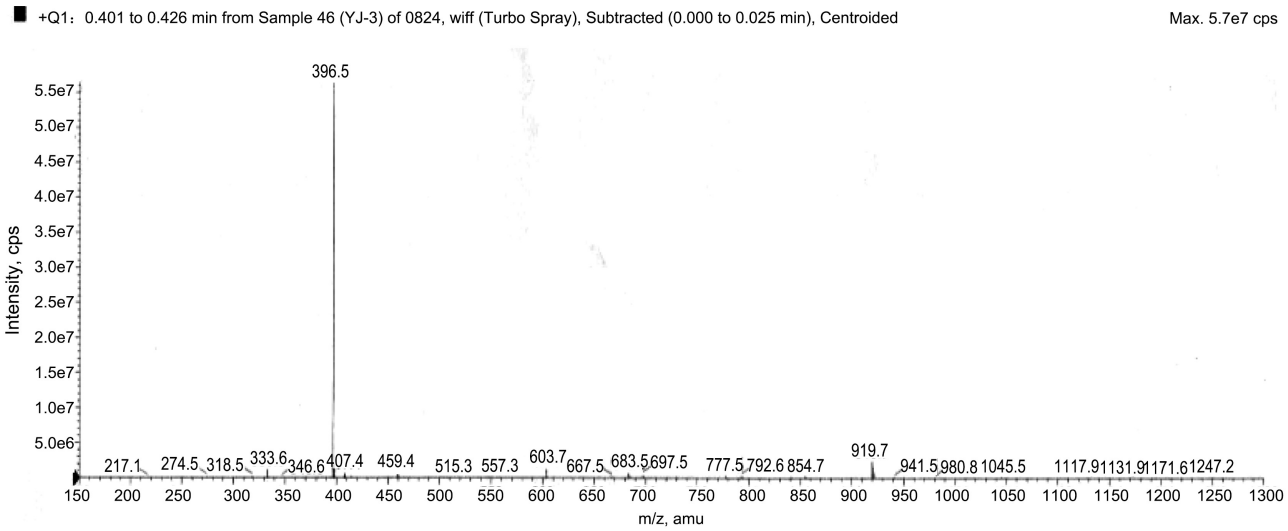

Figure S7. MS spectrum of compound 1a.

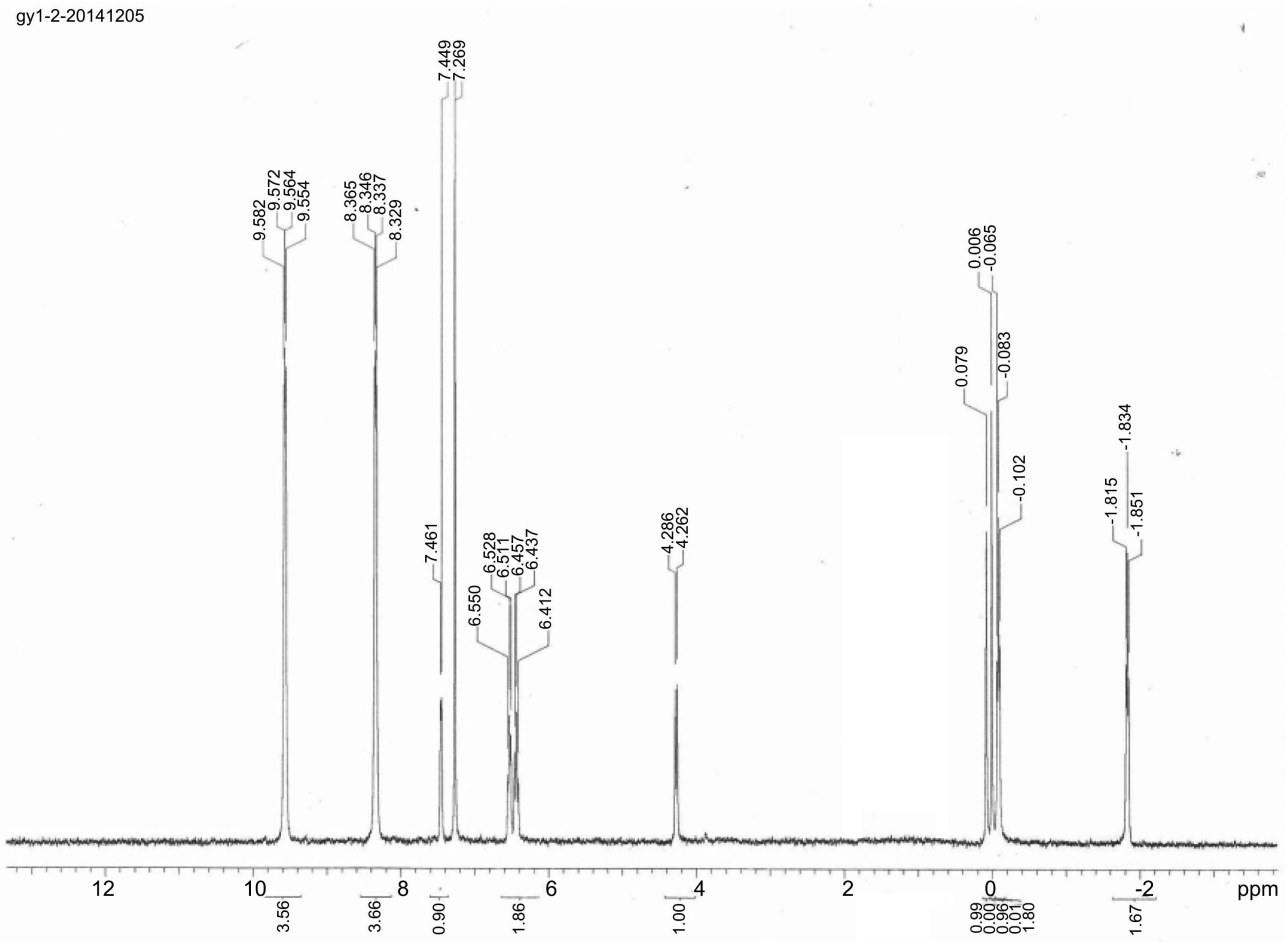

Figure S8. ^{1}H NMR spectrum of compound 2b in $CDCl_3$.

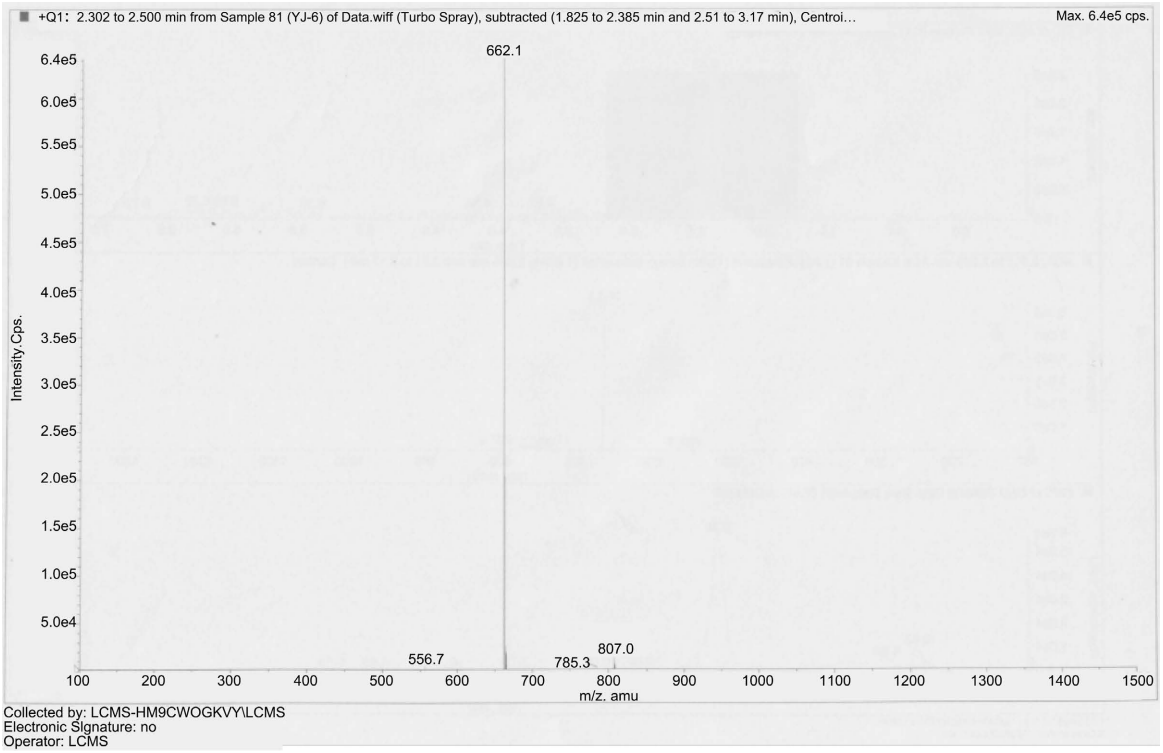

Figure S9. MS spectrum of compound 2b.

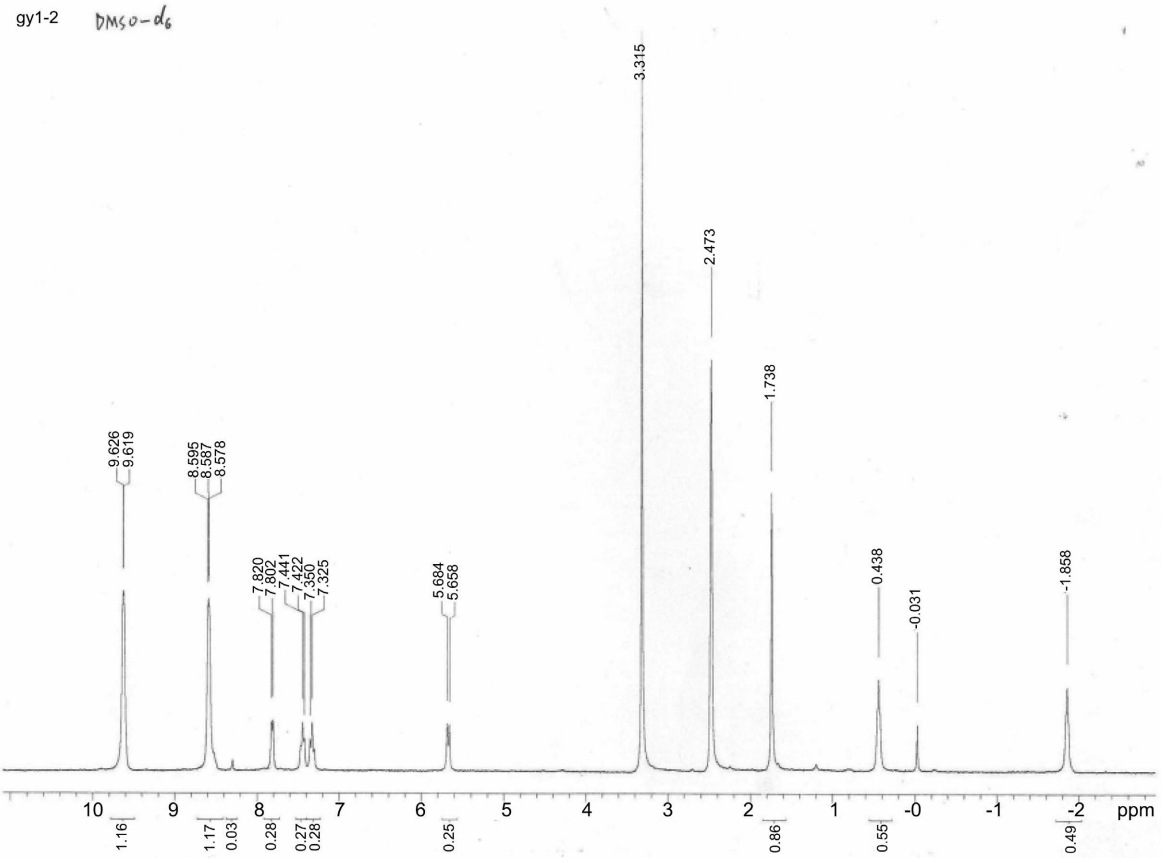

Figure S10. ^{1}H NMR spectrum of compound 1b in DMSO-d_6.

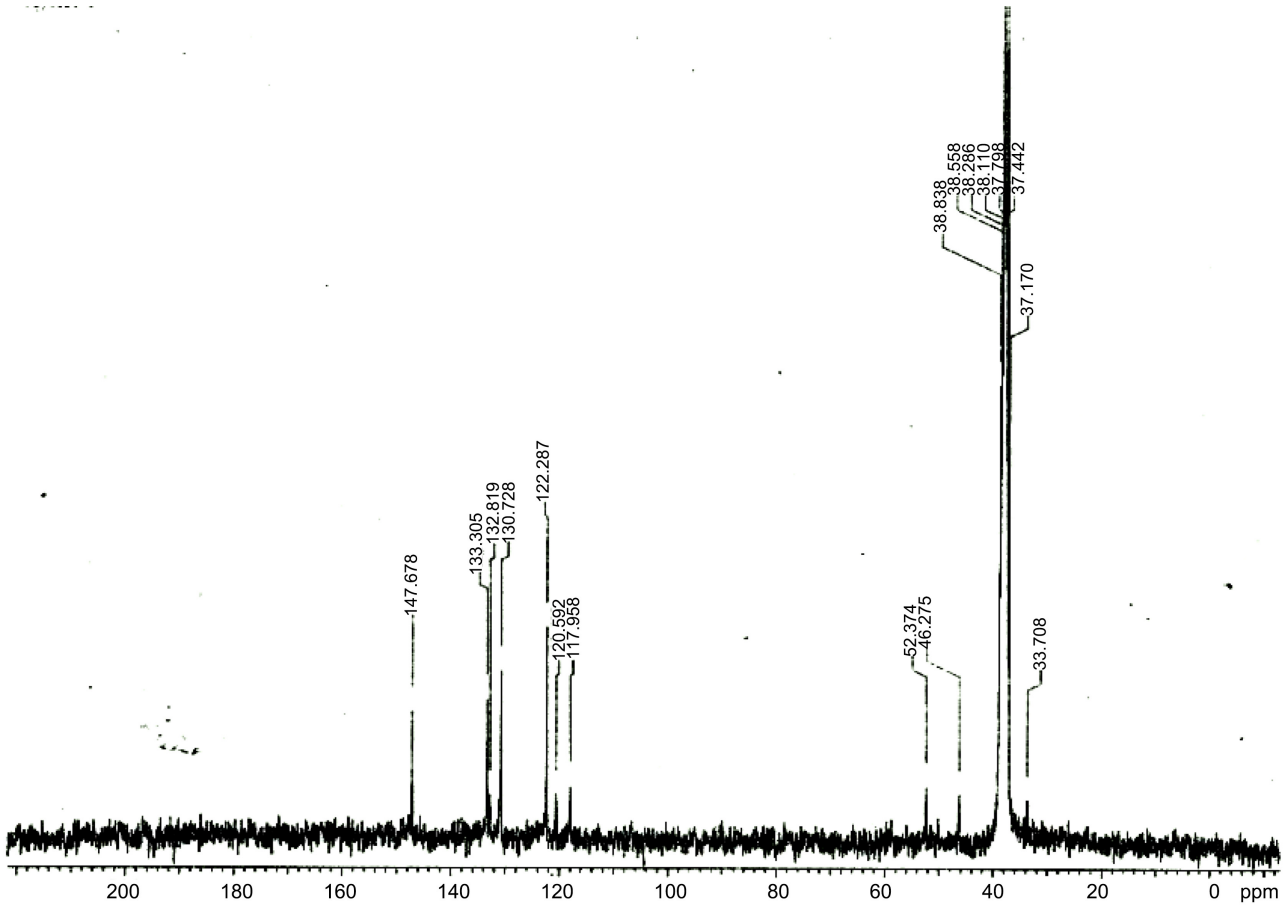

Figure S11. ^{13}C NMR spectrum of compound 1b in DMSO-d_6.

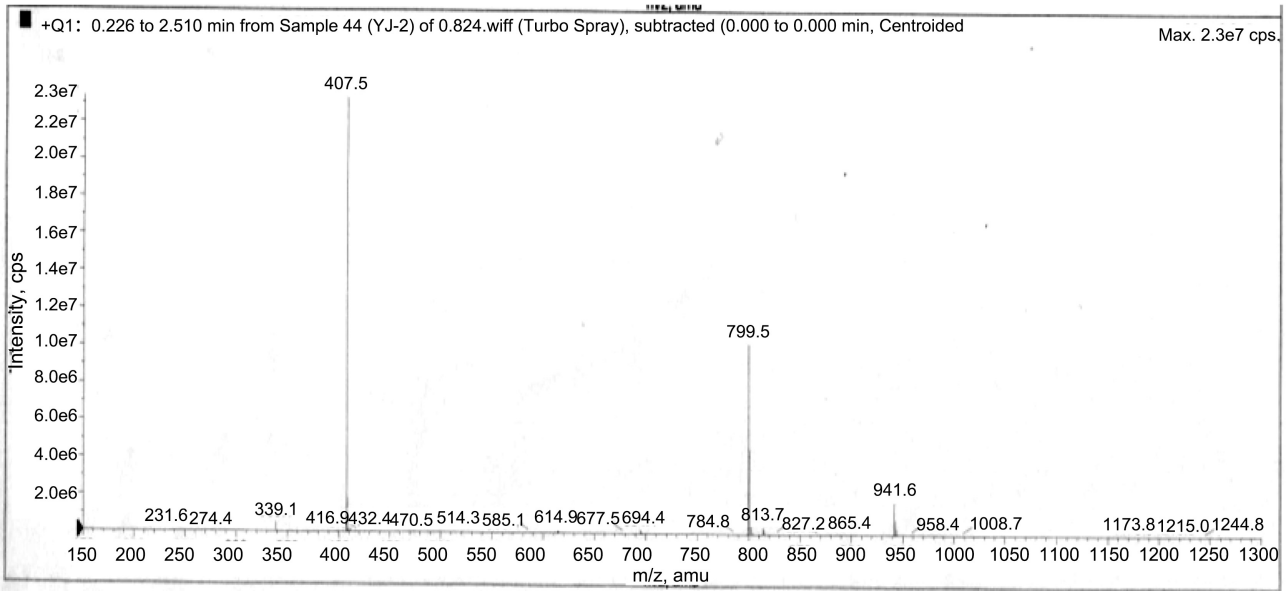

Figure S12. MS spectrum of compound 1b.